

Growth of Well Aligned Tin Oxide Nanotubes by a Sol-gel Method

¹ Mario BIANCHETTI, ² Marjeta MACEK-KRZMANC, ² Sreko D. SKAPIN
and ¹ Noemí E. WALSÖE de RECA

¹ CINSO-CITEDEF-CONICET, Juan Bautista de La Salle 4397, Villa Martelli,
(B1603ALO) Buenos Aires, Argentina

² Advanced Materials Department, Jožef Stefan Institute,
Jamova 39, 1000, Ljubljana, Slovenia

E-mail: walsoe@citedef.gob.ar, marjeta.macek@ijs.si

Received: 24 November 2012 / Accepted: 14 February 2012 / Published: 28 February 2012

Abstract: In previous works, the authors improved the characteristics of resistive gas sensors using SnO₂ nanoparticles to build them. Upon the convenience to increase the surface dimension to enhance the gas absorption area, well aligned SnO₂ nanotubes were prepared by sol-gel method within the pores of a polycarbonate template to increase the sensing surface. To optimize the nanotubes synthesis, some parameters – affecting the nanotubes morphology- were varied and the effects of the different parameters on morphology were compared: the pores size of template membrane, the calcination temperature and time, the precursor solution concentration and the solution aging temperature and time, finding the most convenient conditions to grow the nanotubes. Characterization of nanotubes was performed with XRD being found that the tetragonal rutile was the only crystalline phase exhibited by the polycrystalline nanotubes and their morphology was observed by FE-SEM, discussing the relation among the measured data and the varied parameters affecting the process. *Copyright © 2012 IFSA.*

Keywords: Tin oxide nanotubes, Sol-gel method, Parameters affecting nanotubes growth, Resistive gas sensors.

1. Introduction

Tin oxide (SnO₂) as a stable and n-type large bandgap ($E_g = 3.6$ eV) semiconductor exhibits excellent optical and electrical properties including low resistivity, optical transparency and high theoretical specific capacity. It has been widely used as photocatalyst, gas sensors, glass coatings, solar cells

transparent electrodes and storage applications electrodes. SnO₂ nanomorphologies, exhibit interesting chemical and optoelectronic properties due to their direct channels for efficient electron transport [1-4]. In the last decade, different nanostructured SnO₂ nanorods, nanowires, nanoribbons, nanotubes and nanobelts have been prepared successfully by different techniques [5-8].

Otherwise, the preparation of arrays of well-aligned semiconductor anisotropic nanostructures [9] like nanowires, nanorods or nanotubes, enable to build functional nanodevices like field-effect transistors, electron emitters and electronic and molecular sensing devices. The technical literature also reports few papers about the preparation of SnO₂ arrays of well-aligned one dimensional nanostructure as obtained by sol-gel methods or chemical vapor deposition techniques [10-12]. We shall refer in the following to SnO₂ nanotubes considering that, the usually called nanotubes, do not exhibit nano but microdimensions in spite of being formed by nanoparticles. The aim of this paper was to synthesize SnO₂ nanotubes using a sol-gel technique and polycarbonate templates and the nanotubes were characterized by XRD (X-ray diffraction) and FE-SEM (Field Emission Scanning Electron Microscopy). The effect of the different synthesis parameters on the structure was evaluated and the aspect of nanotubes was observed. The controlled fabrication of well aligned nanotubes for resistive gas sensors, plays an important role to increase the absorption surface of materials for these devices. Resistive gas sensors were already built with nanocrystalline SnO₂ by some authors of this paper [13-17].

2. Experimental

2.1. SnO₂ Nanotubes Preparation

Nanotubes were prepared depositing the desired material by sol-gel within the pores of a template [18, 19]. SnO₂ nanotubes were obtained from SnCl₂.2H₂O and absolute ethanol as starting precursors to get the sol. SnCl₂.2H₂O was dissolved into ethanol to yield solutions with concentrations varying from 0.5 to 1mol/L. At first the alcoxide (ethoxide) is obtained forming the sol by hydrolysis. HCl was added to control the reaction time and the resulting thickness of nanotubes wall. Aging of solution was performed for 2 to 4 h at 80 °C or for long periods (30 days at room temperature). Commercially available template membranes (polycarbonate filters from Millipore) with pores diameter 0.2 μm or 0.8 μm, were used. Membranes were impregnated with the solution creating a pressure variation (by vacuum or over-pressure). Drying was performed by heating at ~ 50 °C for 1 h to remove the solvent and to form the gel and calcination (550 to 750 °C) was performed by a slow heating. Template is removed during the heating process.

2.2. Characterization of SnO₂ Nanotubes

Crystallinity was characterized by X-ray diffraction (XRD) with a Philips PW 3710 diffractometer, using Cu-Kα₁ radiation using as reference: pure cassiterite. In nanomaterials, the spectrum peaks broadening as the particle size decreases is a well known phenomenon [20] and it can be used to determine the particle size (s) by the Scherrer equation:

$$s = k \lambda / \beta \cos \theta,$$

where k is a constant (usually taken as 0.89), λ is the wavelength of the X-ray beam, β is the full width at half maximum height (FWHM) of a given peak (after removal of the instrumental broadening) and θ is the diffracted angle of the peak. Scherrer equation represents the simplest treatment of peak broadening to obtain an average crystallite size As it can be observed in Fig. 1, nanotubes were formed

by crystallites and to determine the crystallites size it was necessary to destroy the nanotubes by milling to separate them.

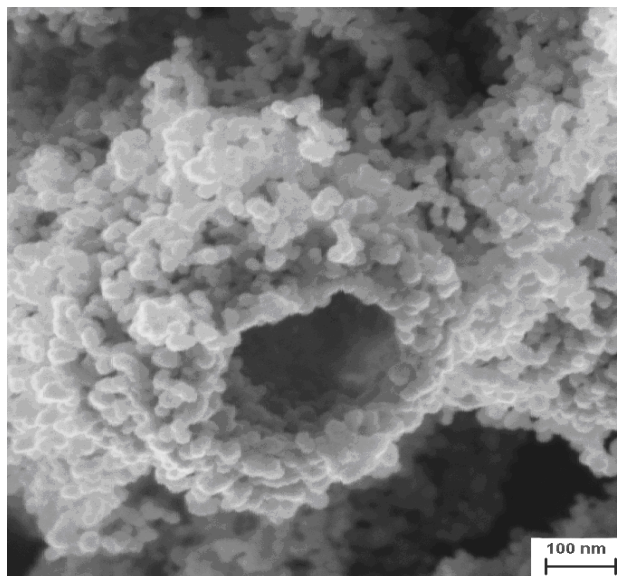


Fig. 1. SnO₂ nanotube.

The general morphology was characterized by Field-Emission Scanning Electron Microscope (FESEM) with a Supra 35VP, Carl-Zeiss Equipment and a FE-SEM, JSM7600, Jeol microscope.

3. Results and Discussion

SnO₂ nanotubes were identified by XRD (X-ray diffraction) showing the tetragonal rutile phase of SnO₂ (JCPDS card, No. 41-1445) with $a = b = 4.738 \text{ \AA}$ and $c = 3.187 \text{ \AA}$ and it was proved that this phase was the only crystalline phase exhibited by the grown nanotubes which were formed by very small size nanoparticles. Every FE-SEM micrograph clearly showed that nanotubes were polycrystalline. The broadening of XRD peaks enabled to calculate the particles size of nanotubes (average size from 20 to 30 nm) using the Scherrer equation. Clearly, this method will only yield an average particle size and it will not provide information on the dispersion of size or the extent of grains agglomeration. Mean size of nanoparticles diameter was corroborated by FE-SEM measurements.

In order to optimize the nanotubes synthesis, some parameters – affecting the nanotubes morphology – were changed leaving fixed the others. In Fig. 1 a hollow nanotube is shown, it is formed by particles being possible that they have grown by the high calcination temperature (750 °C) for 2 h. In this case, polycarbonate template pores diameter was 0.8 μm . Several tubes with the same aspect and dimensions were observed in the surrounding zone, being possible to determine a mean value of tubes length: $(915 \pm 25) \text{ nm}$, tubes diameter: $(860 \pm 42) \text{ nm}$ and wall thickness: $(46 \pm 4.0) \text{ nm}$ (wall thickness measurements were affected by a high error because thickness was very irregular, but measurements were numerous even on the same wall of a tube to determine a real average thickness value). Not only hollow tubes were observed since several of them were half-filled. These dimensions were measured on ten neighbouring nanotubes. The particles diameter varied from $(7.7 \pm 1.0) \text{ nm}$ to $(39 \pm 4.0) \text{ nm}$ with a mean value of particles diameter: $(24 \pm 2.8) \text{ nm}$. Fig. 2 shows a long tube partially broken on its side; the observation of fracture enables to prove that it is a hollow nanotube. Several half filled nanotubes are surrounding it (all of them with similar lengths and diameters). The particles forming the tubes

have grown due to the high calcination temperature: 750 °C for 2 h. The mean nanotubes length was (5230±125) nm, the mean tubes diameter (630±33) nm and the wall thickness varied from (40±4.0) to (50±5.2) nm and the particles diameter changed from (7.6±1.0) nm to (32±3.4) nm, giving a mean particle diameter of (20±2.4) nm. These dimensions were measured on nine neighbouring nanotubes of the same specimen. The unique different parameter was, in this case, the diameter of template hole: 0.2 µm. Early conclusions show that there is a relation between the final diameter and length of nanotubes variations with the template pore diameter, being, at first better to use the membrane with 0.2 µm diameter pores since the tubes length increased and the tubes diameter decreased. In this paper, these results are referred to the micrographs of Figs. 1 and 2 but, results from a dozen a specimen in each case were in agreement for both pores diameter.

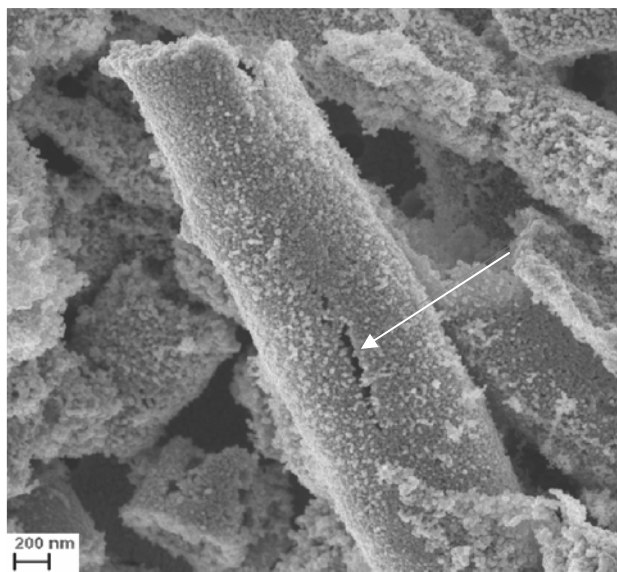


Fig. 2. SnO₂ nanotubes. The arrow points out the fracture in a tube showing that the tube is hollow.

Isolated nanotubes (like the one of Fig. 2) appear together with double fused tubes (shown with arrows in Figs. 3a and 3b) which probably grow through neighbouring pores of template being after stuck. Fig. 4a shows double fused nanotubes and on Fig. 4b, two neighbouring pores of the template are shown. In both cases, nanotubes are nearly filled inside. They are formed by (and, sometimes, partially covered with) particles. The mean particle diameter was 20-25nm in agreement with particles dimensions of Figs. 1 and 2, since the calcination temperature and time were maintained in both cases. Nanotubes were nearly filled with particles and those of Fig. 3a exhibit growth bands (shown by arrows). This probably occurs at the condensation step if drying is too fast. While the template is fused during calcination, the stiffness of the tube sometimes decreases producing its curvature as it is observed in Fig. 5. If calcination temperature is higher, the growth of crystallites is produced as well as the tubes thickness and the diameter of nanotubes (which is related to the membrane pore diameter) also changes. If calcination time (in this case at high temperature) is increased for times ranging from 24 to 50 h, a considerable thickening of nanotubes walls was observed, crystallites size increased and filling of nanotubes was observed in agreement with Shi et al.' results [9]. In case of previous measurements, the precursor solution concentration was maintained at Sn M = 0.5 M. The analysis of parameters variation in a considerable high number of experiments, enabled to fix the optimal calcination conditions: temperature of 550 °C for 24 h.

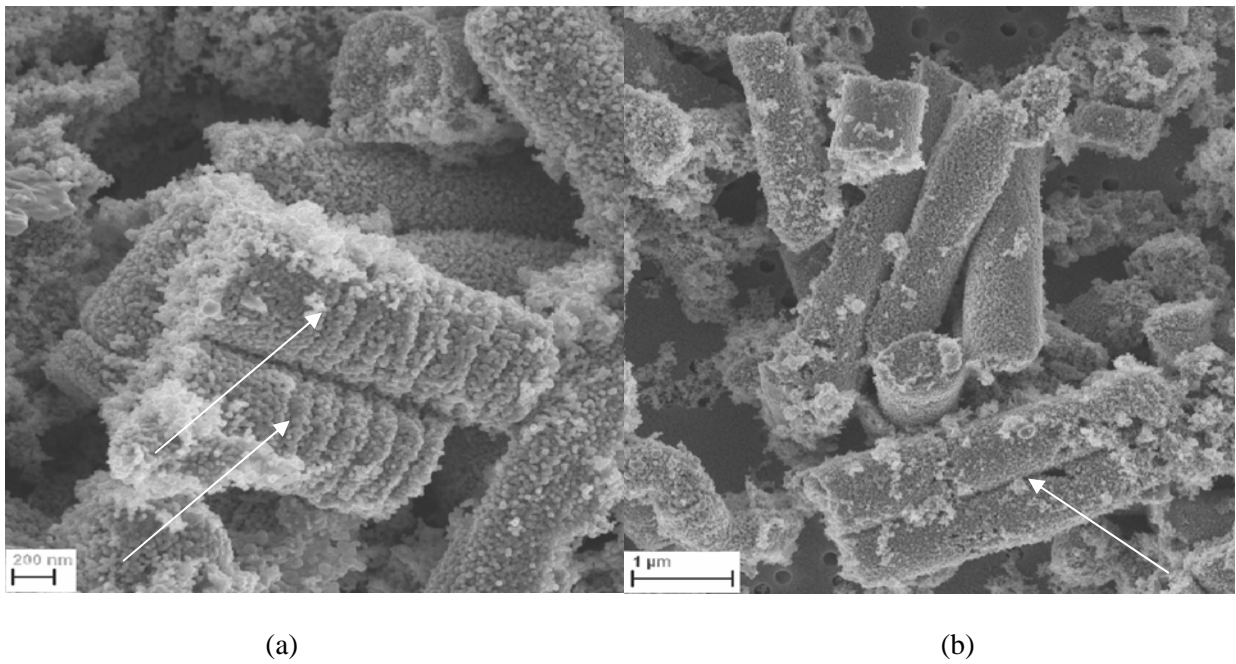


Fig. 3. (a) Fused SnO₂ nanotubes with growth bands; (b) Double fused SnO₂ nanotubes shown by arrows.

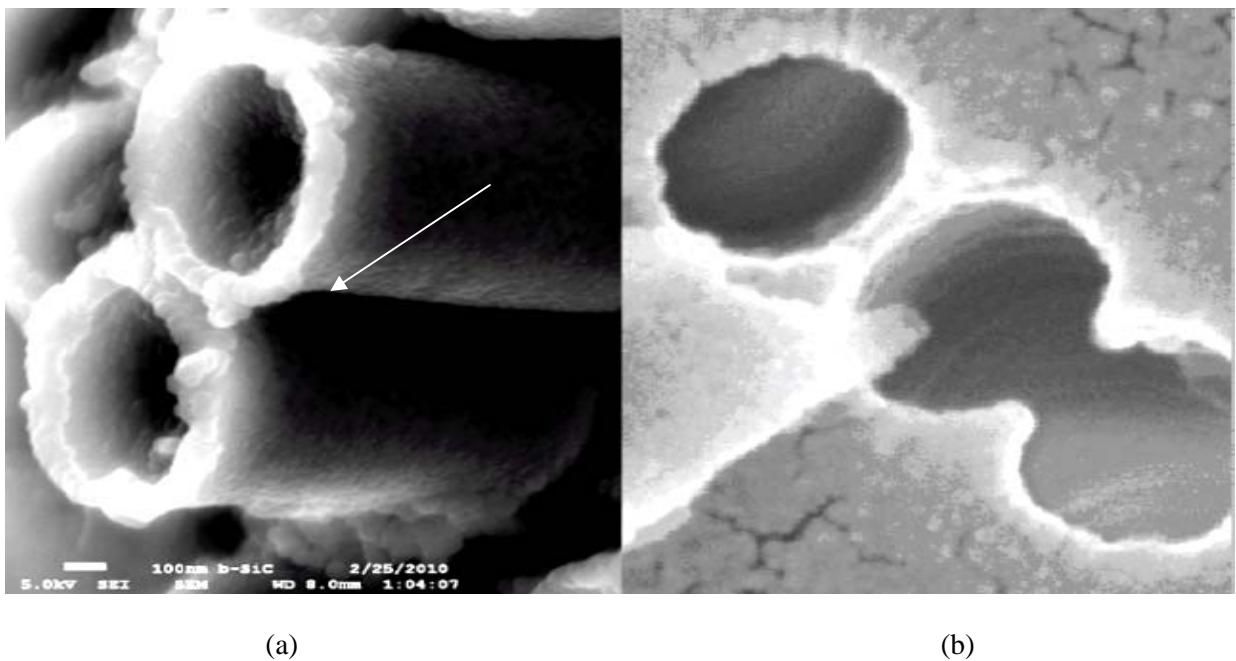


Fig. 4. (a) Double-fused nanotubes; (b) Double pores in polycarbonate template.

The effect of the precursor solution concentration (Sn M) was also taken into account varying it: 2 M, 1.5 M, 1 M, 0.5 M, 0.25 M and 0.18 M after the solution aging at 80°C for 2-4 hours, to evaluate the crystallite size and nanotubes morphology. Micrographs of nanotubes from different precursor solution concentrations (Sn M) showed different morphologies: Fig. 6a (Sn 2M) completely filled tubes with very thick walls, Fig. 6b (Sn 1M) zones with a high quantity of completely filled nanotubes coexisting with partially filled tubes and scarce hollow tubes. Wall thickness of tubes was still thick, Fig. 6c (Sn 0.5M). There were scarce hollow tubes but wall thickness is still large and Fig. 6d Sn 0.18M) large zones with parallel grown nanotubes which walls thickness is homogeneously thin.

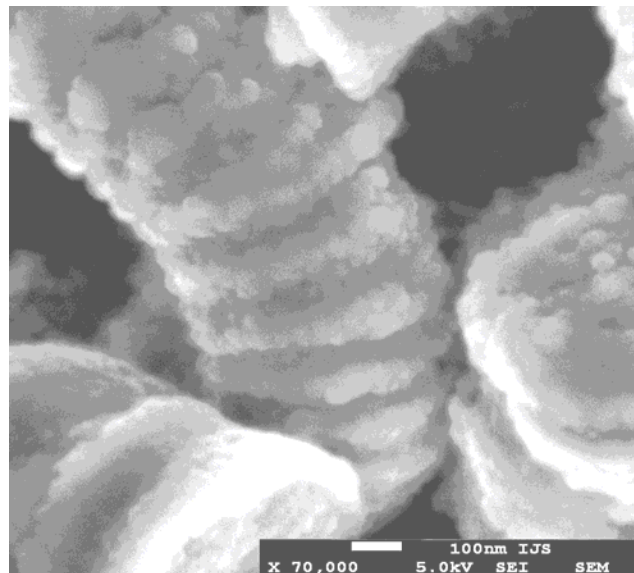


Fig. 5. Curved SnO₂ nanotube with growth bands.

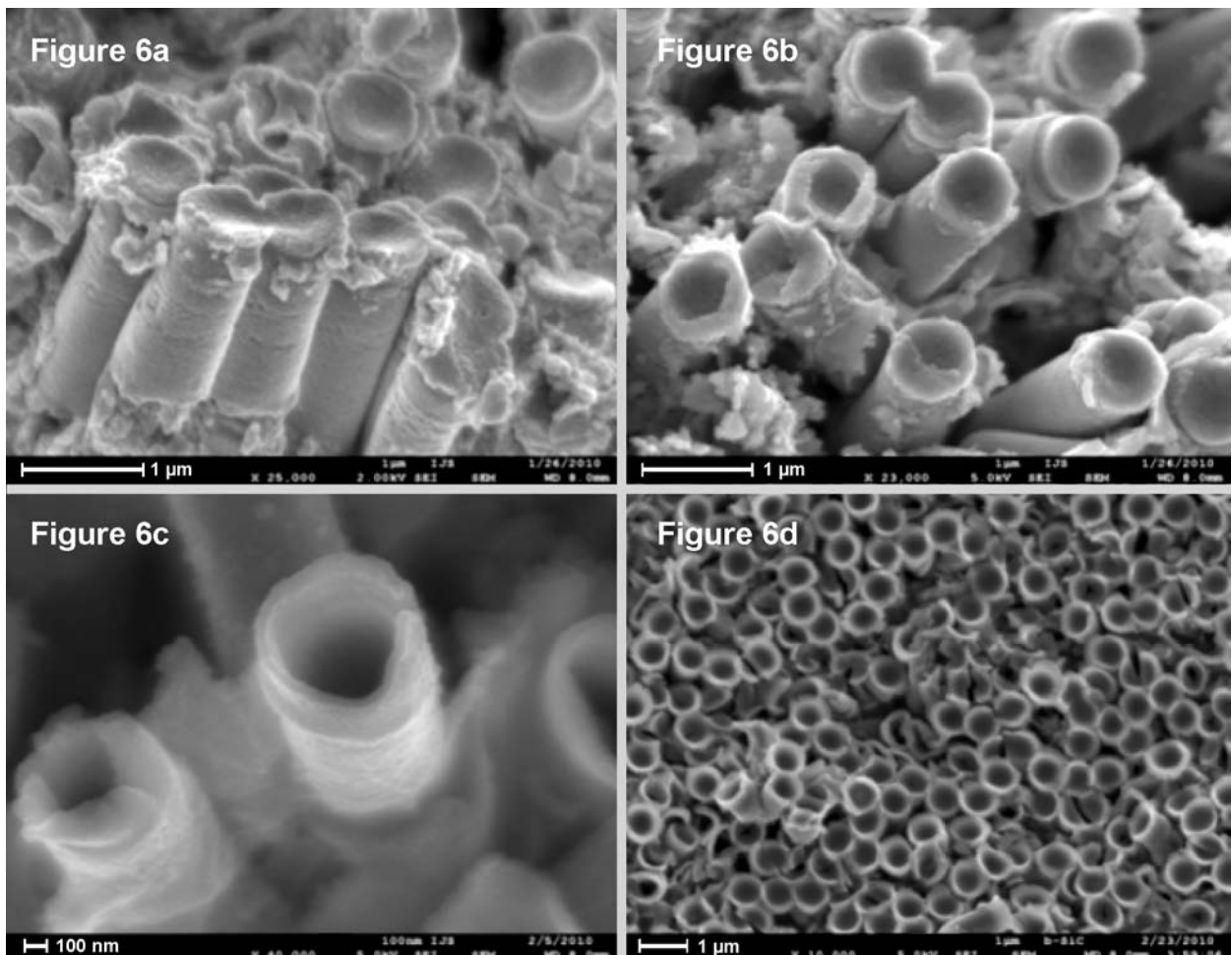


Fig. 6. (a) Precursor solution concentration Sn 2 M; (b) Precursor solution concentration Sn 1 M; (c) Precursor solution concentration Sn 0.5 M; (d) Precursor solution concentration Sn 0.18 M.

The parameter which was taken into account is the aging temperature and time. Sets of specimen were obtained at different lower concentrations (Sn M) of the precursor solution (0.68 M, 0.41 M, 0.27 M,

0.18 M and 0.12 M) and aging of thirty days at room temperature. Measurements of specimen characteristics: tubes length (μm), tubes diameter (nm), tubes wall thickness (nm) and crystallites diameter (nm) enabled to plot these parameters versus the composition (Sn M) (Figs. 7A to 7D). A careful review of Figs. 7 data and the observation of HRTEM micrographs of the same specimen enabled to conclude that for 30 days aging at room temperature the most convenient concentration (Sn M) of precursor solution was always in the range from 0.12 to 0.18 M). Figs. 8a and 8b show: well aligned, fine and hollow nanotubes, homogeneous in size and formed by small crystallites. As the precursor solution concentration increased, i.e. at the 0.27 M, many nanotubes appear to be filled (Fig. 9a) and their aligned growth began to be disordered in some zones. These effects increased at larger concentrations: in Fig. 9a, some filled nanotubes are shown prepared with a precursor solution concentration of Sn 0.27 M, being the aging maintained at room temperature for 30 days. For the same conditions (with exception of the precursor solution concentration in this case: Sn 0.41 M) nearly all the nanotubes were completely filled and growth ordering was lost (Fig. 9b) and finally for the higher precursor solution concentration (Sn 0.68 M), the most of nanotubes were filled and growth ordering was completely lost (Fig. 9c). The precursor solution concentration was measured immediately before the preparation of nanotubes to avoid evaporation effects during aging. Taking into account the minimal and maximal limits of aging: 80°C for two hours and room temperature for 30 days, it is possible to conclude that the lower concentrations (0.12 M and 0.18 M) enabled to build well aligned nanotubes with excellent characteristics. Possibility of preparing larger nanotubes (in length and diameter) enabling larger surfaces and, consequently, a higher absorption of gases was considerably affected by the presence of disordered and filled tubes with the subsequent reduction of the absorption surface.

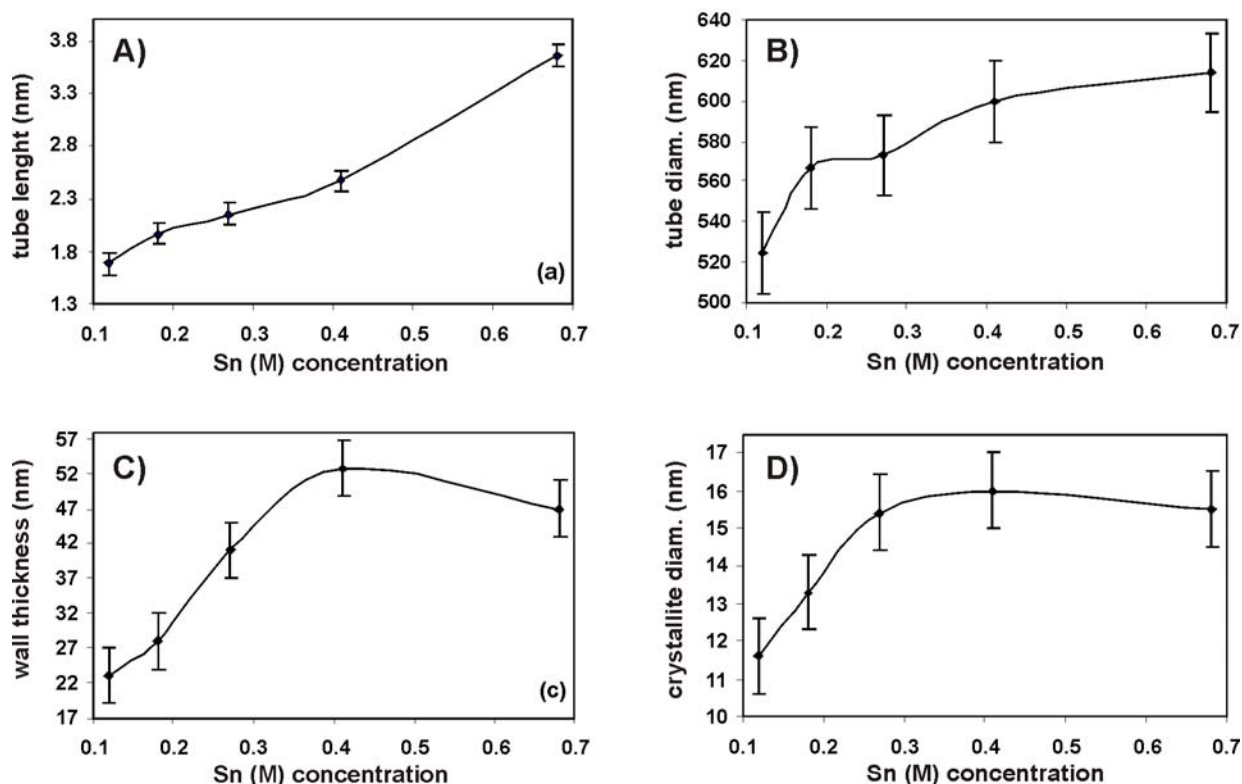


Fig. 7. (a) Nanotubes length (μm) vs. molar Sn concentration; (b) Nanotubes diameter (μm) vs. molar Sn concentration; (c) Tubes wall thickness (nm) vs. molar Sn concentration, (d) crystallites diameter (nm) vs. molar Sn concentration.

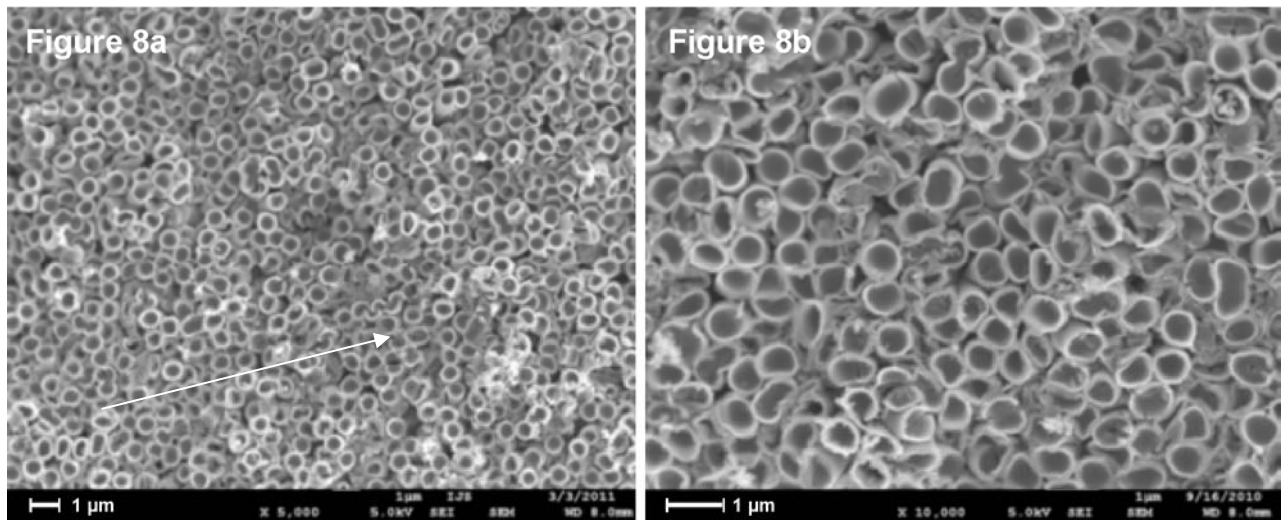


Fig. 8. (a) Precursor solution concentration Sn 0.12 M. Aging at room temperature for 30 days; (b) Precursor solution concentration (Sn 0.18 M). Aging at room temperature for 30 days.

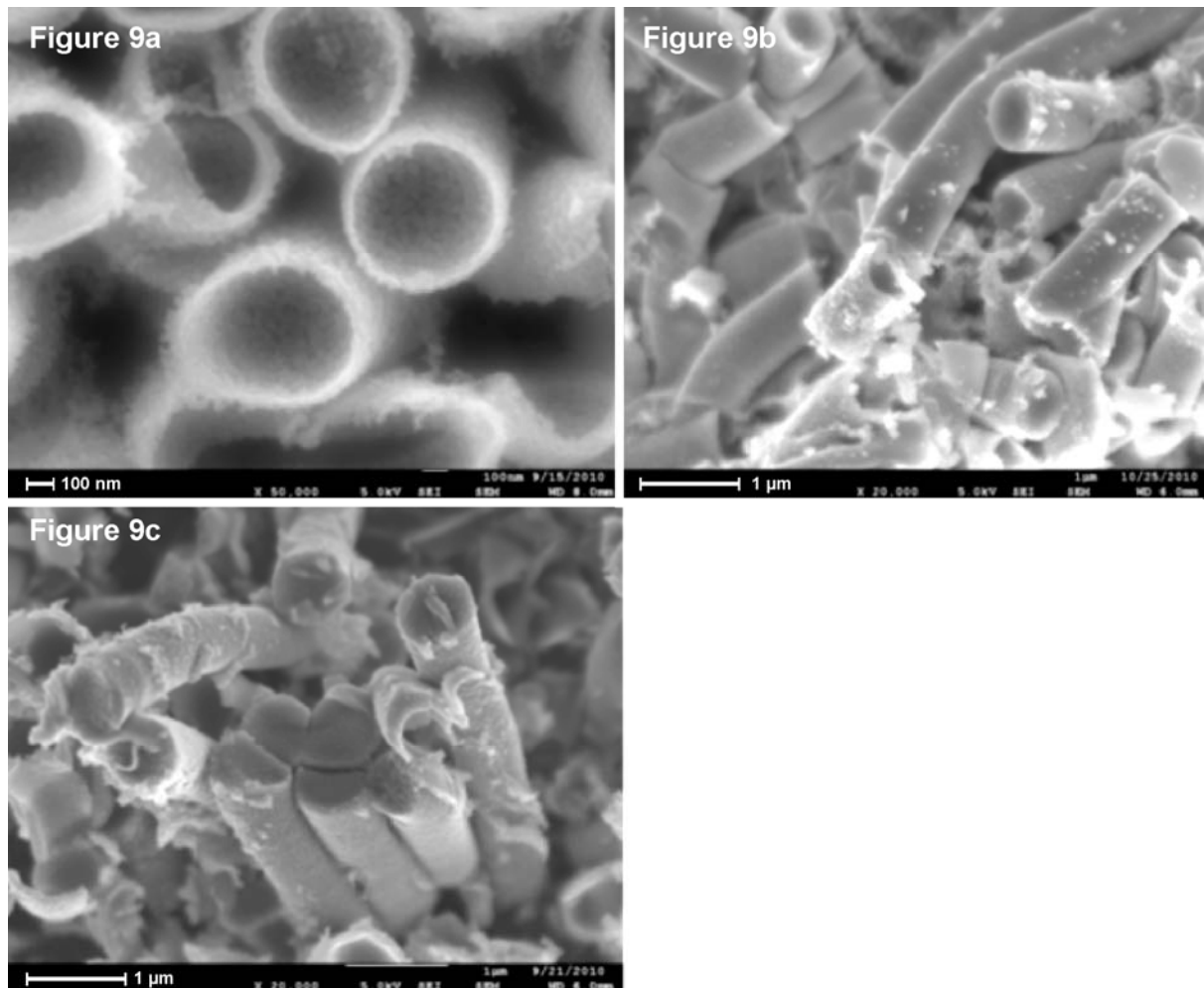


Fig. 9. (a) Some nanotubes are nearly filled. Precursor solution concentration (Sn 0.27 M). Aging at room temperature for 30 days; (b) Some nanotubes were completely filled and growth ordering was lost. Precursor solution concentration (Sn 0.41 M). Aging at room temperature for 30 days; (c) Nanotubes were completely filled and growth ordering was lost. Precursor solution concentration (Sn 0.68M). Aging at room temperature for 30 days.

Conclusions

SnO₂ nanotubes were prepared depositing the desired material by sol-gel within the pores of templates with different pores diameter. Nanotubes were identified by XRD proving that the tetragonal rutile phase of SnO₂ was the only crystalline phase exhibited by the grown polycrystalline nanotubes. Tubes were formed by very small size nanoparticles (from 20 to 30 nm) as it was proved by XRD (Scherrer equation) and by FE-SEM observations.

In order to optimize the nanotubes synthesis, some parameters – affecting the nanotubes morphology – were changed leaving fixed the others with the purpose to apply the material for gas sensors trying, in consequence, to increase the surface and the gases absorption area. The effect of different parameters on the nanotubes morphology was considered and their influence on resulting characteristics of nanotubes was measured: the pores size of template membrane (0.2 and 0.8 μm), calcination temperature 550 to 750 °C and time (24 to 50 h), precursor solution concentration and aging time (from Sn 0.12 M to Sn 5M) and solution aging temperature and time, from 2h at 80 °C to 30 days at room temperature) finding the most convenient conditions to reach the proposed objectives. The morphology of tubes was observed by FE-SEM, being discussed and compared with measured data of the affecting parameters.

Acknowledgements

The authors are indebted to CONICET by the Grant PIP Ner. 1122-00901-00355 (2010/13) granted for this research and to Eng. Ma. Emilia. F. de Rapp and Fernando Vázquez Rovere by their valuable assistance in XRD analysis and drawings and design, respectively.

References

- [1]. Y. Xia, P. Yang, Y. Sun, Y. Wu, B. Mayers, B. Gates, Y. Yin, F. Kim, H. Yan, One-dimensional nanostructures: synthesis, characterization, and applications, *Adv. Mater.*, 15, 2003, pp. 353-389.
- [2]. D. Wang, X. F. Chu, M. L. Gong, Gas-sensing properties of sensors based on single-crystalline SnO₂ nanorods prepared by a simple molten-salt method, *Sensors & Actuators B*, 117, 2006, pp. 183–187.
- [3]. N. Du, H. Zhang, B. D. Chen, X. Y. Ma, Z. H. Liu, J. B. Wu, D. R. Yang, Porous indium oxide nanotubes: Layer-by-layer assembly on carbon-nanotube templates and application for room-temperature NH₃ gas sensors, *Adv. Mater.*, 19, 2007, pp. 1641-1645.
- [4]. G. Xi, J. H. Ye., Ultrathin SnO₂ nanorods: template- and surfactant-free solution phase synthesis, growth mechanism, optical, gas-sensing, and surface adsorption properties, *Inorg Chem.*, 49, 5, 2010, pp. 2302-2309.
- [5]. Y. Wang, X. C. Jiang, Y. Xia, A Solution-Phase, precursor route to polycrystalline SnO₂ nanowires that can be used for gas sensing under ambient conditions, *J. Am. Chem. Soc.*, 125, 2003, pp. 16176–16177.
- [6]. H. G. Yang, H. C. Zeng, Self-construction of hollow SnO₂ octahedra based on two-dimensional aggregation of nanocrystallites, *Angewandte Chemie International Edition*, 43, 2004, pp. 5930-5933.
- [7]. L. Zhao, M. Yosef, M. Steinhart, P. Göring, H. Hofmeister, U. Gösele, S. Schlecht, Porous silicon and alumina as chemically reactive templates for the synthesis of tubes and wires of SnSe, Sn, and SnO₂, *Angewandte Chemie International Edition*, 45, 2005, pp. 311-315.
- [8]. J. Liu, F. Gu, Y. Hu, C Li, Flame synthesis of tin oxide nanorods: A continuous and scalable approach, *J. Phys. Chem. C*, 114, 13, 2010, pp. 5867–5870.
- [9]. L. Shi, Y. Xu, Q. Li, Controlled fabrication of SnO₂ arrays of well-aligned nanotubes and nanowires, *Nanoscale*, 2, 2010, pp. 2104-2108.
- [10]. N. Zhao, G. Wang, Y. Huang, B. Wang, B. Yao, Y. Wu, Preparation of nanowire arrays of amorphous carbon nanotube-coated single crystal SnO₂, *Chem. Mater.*, 20, 8, 2008, pp. 2612–2614.
- [11]. Y. Liu and M. Liu, Growth of aligned square-shaped SnO₂ tube arrays, *Adv. Funct. Mater.*, 15, 2005, pp. 57–62.

- [12].M. Liu, J. Dong and Y. Liu, Well Aligned Nano- “Box Beams”, of SnO₂, *Adv. Funct. Mater.*, 16, 2004, pp. 353-356.
- [13].L. B. Fraigi, D. G. Lamas, N. E. Walsøe de Reca, *Microsensores de Estado Sólido para Monitoreo de Medio Ambiente*, Programa CYTED (Ciencia y Tecnología para el Desarrollo), Proyecto IX. 2, Ed. Control S. R. L., Bs. As., 1999, pp. 57-72.
- [14].L. B. Fraigi, Sensores de CO (g) basados en óxido de estaño nanoestructurado, Doctoral Thesis (Engineering), *FI-Universidad de Buenos Aires*, 2006.
- [15].N. E. Walsøe de Reca, Nanostructured Materials, *Anales Academia Nacional de Ciencias Exactas, Físicas y Naturales*, 59, 2007, pp. 59-93.
- [16].M. F. Bianchetti, N. E. Walsøe de Reca, A Sensor built with nanocrystalline SnO₂ to detect hydrogen, Application for A. R. Patent (in process).
- [17].L. T. Alaniz, C. L. Arrieta, M. F. Bianchetti, C. A. Gillari, J. F. Giménez, H. A. Lacomí, D. F. Valerio and N. E. Walsøe de Reca, Gas sensor with microheating device by direct contact and sensing method, A. R. Patent PP-070105987, granted on 28/12/2007.
- [18].N. Li and C. R. Martin, A high-rate, high-capacity, nanostructured Sn-based anode prepared using Sol-Gel template synthesis, *J. Electrochem. Soc.*, 148, 2001, pp. A164-A170.
- [19].W. Zhu, W. Wang, H. Xu, J. Shi, Fabrication of ordered SnO₂ nanotube arrays via a template route, *Materials Chem. Phys.*, 99, 2006, pp. 127-130.
- [20].H. P. Klug, L. E. Alexander, X-Ray Diffraction Procedures for polycrystalline and amorphous Materials, *Wiley Interscience Publication*, New York, 1974.
- [21].D. Balzar, Defect and Microstructure Analysis from Diffraction, *Oxford University Press*, London, New York, 1999.

2012 Copyright ©, International Frequency Sensor Association (IFSA). All rights reserved.
(<http://www.sensorsportal.com>)

Universal Sensors and Transducers Interface (USTI)

for any sensors and transducers with frequency, period, duty-cycle, time interval, PWM, phase-shift, pulse number output



- * Input frequency range:
0.05 Hz ... 9 MHz (144 MHz)
- * Selectable and constant relative error:
1 ... 0.0005 % for all frequency range
- * Scalable resolution
- * Non-redundant conversion time
- * RS232, SPI, I2C interfaces
- * Rotational speed, rpm
- * Cx, 50 pF to 100 μF
- * Rx, 10 Ω to 10 MΩ
- * Pt100, Pt1000, Pt5000, Cu, Ni
- * Resistive Bridges
- * PDIP, TQFP, MLF packages

Just make it easy !

<http://www.techassist2010.com/> info@techassist2010.com